



## Research article

## 3D cone-beam CT of the ankle using a novel twin robotic X-ray system: Assessment of image quality and radiation dose



Jan-Peter Grunz<sup>a,\*</sup>, Andreas Steven Kunz<sup>a</sup>, Carsten Herbert Gietzen<sup>a</sup>, Andreas Max Weng<sup>a</sup>,  
Maike Veyhl-Wichmann<sup>b</sup>, Süleyman Ergün<sup>b</sup>, Rainer Schmitt<sup>a,c</sup>, Thorsten Alexander Bley<sup>a</sup>,  
Tobias Gassenmaier<sup>a</sup>

<sup>a</sup> Department of Diagnostic and Interventional Radiology, University Hospital Würzburg, Würzburg, Germany

<sup>b</sup> Institute of Anatomy and Cell Biology, University of Würzburg, Würzburg, Germany

<sup>c</sup> Department of Diagnostic and Interventional Radiology, Cardiovascular Center Bad Neustadt an der Saale, Bad Neustadt an der Saale, Germany

## ARTICLE INFO

## Keywords:

Twin robotic X-ray system  
Cone-beam computed tomography  
Computed tomography  
Ankle  
Radiation dosage

## ABSTRACT

**Purpose:** To evaluate image quality (IQ) and radiation dose in cone-beam computed tomography (CBCT) of the ankle using a novel twin robotic X-ray system.

**Method:** We examined 16 cadaveric ankles with standard-dose (FD) and low-dose (LD) protocols using the new system's CBCT mode. For comparison, we performed multi-slice CT imaging (MSCT) with a clinical protocol. Three radiologists assessed IQ, noise and artifacts in bone and soft tissue on a five-point Likert scale (1 = poor IQ; strong noise or artifacts; 5 = excellent IQ; minimal noise or artifacts). Volume CT dose indices (CTDI<sub>vol</sub>) were calculated for radiation dose comparison between CBCT and MSCT.

**Results:** Overall IQ was described as very good or excellent by reader 1/2/3 in 62.5/87.5/56.3% of LD, 87.5/87.5/81.3% of FD and 100/87.5/87.5% of MSCT studies. Readers agreed that IQ was better in MSCT than LD (R1/R2/R3;  $p \leq 0.008$ ), two also found advantages of MSCT over FD (R1/R3;  $p \leq 0.034$ ). Soft tissue noise and artifacts were stronger in FD (all  $p \leq 0.002$ ) and LD (all  $p \leq 0.001$ ). In bone, artifacts and noise were also more severe in LD (all  $p < 0.001$ ) and FD (all  $p \leq 0.003$ ). CTDI<sub>vol</sub> for clinical MSCT scans without dose modulation ( $15.0 \pm 0.0$  mGy) were higher than for FD ( $5.3 \pm 1.0$  mGy) and LD studies ( $2.9 \pm 0.6$  mGy; both  $p < 0.001$ ).  
**Conclusions:** Despite MSCT providing better overall IQ than the twin robotic X-ray system's CBCT mode, both cone-beam protocols offer very good IQ in most studies and are suitable for clinical ankle imaging. Standard-dose and especially low-dose CBCT studies deliver up to five times less radiation dose than MSCT imaging.

## 1. Introduction

Acute ankle sprain is a common trauma-related diagnosis and accounts for approximately 3–5% of all emergency rooms attendances in the UK [1]. Oftentimes, serious injuries of the foot and ankle region occur by falling from heights or involvement in traffic accidents, resulting in ligament and/or bone damage. Fractures of the lower extremity hold particular socioeconomic relevance as they amount to almost 10% of all fractures in humans [2]. Reporting incidences of 9/1000 per year and increased prevalence in patients aged 50 years or older [3], malleolar fractures are among the most common imaging tasks in radiology departments. From an individual perspective, they

frequently require long periods of rehabilitation or surgical treatment, sometimes leading to permanent limitation of mobility [4]. In acute trauma, plain radiography is the primary means of fracture diagnosis, as it provides fast and cost-effective imaging at a favorable radiation dose. However, in case of complex fracture patterns, the injury extent might be obscured in conventional radiographs due to overlapping osseous structures. To provide more precise information regarding the exact location of fragments, computed tomography may be necessary [5]. Surgical planning profits in particular from the advantages of CT, as surgeons can devise their interventions on multidimensionally reconstructed images [6].

Many hospitals use multi-slice computed tomography (MSCT)

**Abbreviations:** CBCT, cone-beam computed tomography; FD, CBCT protocol with a standard-dose level; LD, CBCT protocol with a dedicated low-dose level; MSCT, multi-slice computed tomography; CTDI<sub>vol</sub>, volume computed tomography dose index; DAP, dose-area product; DLP, dose-length product

\* Corresponding author at: Department of Diagnostic and Interventional Radiology, University Hospital Würzburg, Oberdürrbacher Straße 6, 97080, Würzburg, Germany.

E-mail address: [Grunz\\_J@ukw.de](mailto:Grunz_J@ukw.de) (J.-P. Grunz).

<https://doi.org/10.1016/j.ejrad.2019.108659>

Received 12 June 2019; Received in revised form 3 September 2019; Accepted 4 September 2019

0720-048X/© 2019 Elsevier B.V. All rights reserved.

technology for their 3D musculoskeletal imaging tasks. Nonetheless, the benefits of MSCT imaging often come at the price of additional radiation dose [7]. One approach to ensure diagnostic 3D image quality while also keeping the dose level “as low as reasonably achievable” (ALARA), is to implement cone-beam computed tomography (CBCT) for extremity imaging [8]. For a long time, CBCT has been used extensively in dentomaxillofacial radiology because of its excellent depiction of bone structures at minimized radiation doses [9–11]. In the last decade, the emergence of dedicated CBCT extremity scanners has resulted in cone-beam technology being increasingly present in musculoskeletal imaging as well [12,13]. While there are several advantages to the examination of injured wrists (e.g. positioning options), the true potential of CBCT scanners becomes evident when performing lower extremity or spine imaging, as some systems feature the option to scan articular joints or vertebral bodies under weight-bearing conditions [14,15]. This option is particularly important because joint depiction, for instance, varies considerably depending on the axial load [16,17].

Due to general lack of data regarding the performance of its 3D CBCT scan mode, this study’s purpose was to provide a first evaluation of a new twin robotic X-ray system’s CBCT image quality and radiation dose in cadaveric ankle imaging under lying conditions and compare the results to MSCT.

## 2. Material and methods

### 2.1. Cadaveric specimens

Eight cadaveric specimens were obtained from the Institute of Anatomy and Cell Biology, University of Würzburg, Germany. A total number of 48 examinations were performed (16 FD, 16 LD, 16 MSCT studies) with the subjects in horizontal position. Depending on the cadavers’ hip and knee joint flexibility, MSCT scans were either conducted with the opposite leg bent at an angle of approximately 90 degrees (“single foot”, 10 of 16 ankle scans) or both feet positioned in parallel fashion (“parallel feet”, 6 of 16 ankle scans). CBCT examinations were carried out with single foot or parallel feet positioning accordingly to MSCT. The single foot positioning for 3D CBCT and MSCT imaging is depicted in Fig. 1.

### 2.2. Scanners

Image quality and radiation dose were assessed with a novel multifunctional X-ray system with implemented 3D CBCT mode (Multitom Rax, Siemens Healthineers, Erlangen, Germany). The system possesses

two motor-driven telescopic arms with one arm carrying the X-ray tube and the other being equipped with a 42.6 x 42.6 cm flat panel detector. Both arms have several degrees of freedom for 2D and fluoroscopy scans, allowing for independent movement to predefined positions in the exam room. Simultaneous arm movement along predefined scanning trajectories enables acquisition of 3D projection data for cone-beam CT reconstruction. For lower extremity imaging, a scan trajectory around the patient table is used with a sweep angle of 183° and source-to-image-distance of 105 cm. The X-ray tube is capable of currents between 0.5 and 800 mAs, and voltages between 40 and 150 kVp. Irrespective of scan trajectory, overall scan time is 20 s with 16 frames per second and 23 cm field of view at maximum. Acceleration and deceleration phase at the beginning and end of image acquisition result in a total of 298 projection images per scan. The scans in this study were performed with the commercially available software version VF10.

For performance comparison, a conventional MSCT scanner from clinical routine was employed (Somatom Definition AS, Siemens Healthineers, Erlangen, Germany).

### 2.3. Scan protocols

Before 3D CBCT imaging is commenced, target dose values can be selected in the system settings. In CBCT mode, a sensor contained by the X-ray detector measures the incoming radiation continuously, whereupon the system uses automatic dose regulation to maintain the detector dose according to the predetermined dose level. Therefore, the tube-current-time product is adjusted after every projection image.

We used two different CBCT scan protocols for this study, one with a dose level of 0.4–0.7 (low-dose protocol, LD), the other with a dose level of 0.7–1.4 (standard-dose protocol, FD). Adhering to the preset dose level, the mean total tube current per ankle scan was  $191.4 \pm 36.2$  mAs for FD and  $121.6 \pm 17.7$  mAs for LD studies. The system operated at 78.9 kVp for all examinations and the built in 0.3 mm copper filter was in effect during every scan.

Using single-energy mode, the conventional MSCT scans were performed with a clinical protocol consisting of reference tube voltage of 120 kVp and tube current of 100 mAs. Detector collimation was 64 x 0.6 mm and pitch factor 0.8. Adhering to the clinical protocol, automatic tube current modulation was deactivated.

### 2.4. Dose assessment

For radiation dose estimation in MSCT, we recorded dose-length products (DLP) and volume computed tomography dose indices



Fig. 1. Scan positions.

Single-foot positioning options for ankle imaging using the twin robotic X-ray system (right) and conventional multi-slice computed tomography (left). Feet can also be positioned together in parallel fashion if hip and knee joint mobility is limited.



**Fig. 2.** Image quality.

Illustration of overall image quality in ankle imaging by representative CBCT and MSCT slices. Left column: coronal MPR of (a) FD, (b) LD, (c) MSCT scans. Right column: sagittal MPR of (d) FD, (e) LD, (f) MSCT scans.

( $CTDI_{vol}$ ). To enable dosage comparison, dose-area product (DAP) values were recorded in 3D CBCT ankle imaging. Through multiplication by a preset linear scaling factor, we received  $CTDI_{vol}$ -equivalent values for our cone-beam examinations. This factor was determined in advance for every combination of acquisition geometry, dose level and tube voltage. For this purpose, we used a commercially available dosimetry system (Nomex Dosimeter, PTW, Freiburg, Germany) with a 30 cm ionization chamber in combination with a PMMA dosimetry

phantom compliant with IEC 60601-2-44:2009. The phantom features a diameter of 16 cm and total length of 30 cm. After DLP measurements in each of five chambers, standard weighting schemes for dose measurement were utilized on the chambers' values to assess  $DLP_{vol}$  values. In order to compute the corresponding  $CTDI_{vol}$ ,  $DLP_{vol}$  values were divided by the beam width, which is equivalent to the field of view in z-direction. For conclusive calculation of the scaling factor,  $CTDI_{vol}$  was divided by DAP.

## 2.5. Image reconstruction

Irrespective of scan protocol and imaging modality, all image reconstructions were carried out with identical parameters using dedicated software (syngo via, Siemens Healthineers, Erlangen, Germany). We reconstructed axial, coronal and sagittal planes with slice thickness of 1.0 mm, increment of 0.5 mm, image matrix of  $1024 \times 1024$  pixels and field of view of 80 mm. Window width and center were set to 3000 and 1000 HU for bone depiction; however, observers were allowed to alter window width and center for their reads.

## 2.6. Image analysis

Three independent radiologists with eight (R1), three (R2) and five (R3) years of experience in musculoskeletal imaging evaluated all scans in randomized and blinded fashion using dedicated PACS software (Merlin, Phönix-PACS). After blinded initial review of all images, each observer then assessed whether they considered image quality sufficient for diagnostic use. Secondly, they rated overall image quality, image noise and artifacts for bone and soft tissue using a five-point Likert scale (5 = excellent image quality, minimal noise or artifacts; 4 = very good image quality, little noise or artifacts; 3 = moderate image quality, noise or artifacts; 2 = fair image quality, considerable noise or artifacts; 1 = poor image quality, strong noise or artifacts).

## 2.7. Statistics

Statistical analyses were carried out with dedicated software (SPSS Statistics Version 23.0 for Mac, IBM, Armonk, New York, USA). Categorical variables are presented as frequencies and percentages. Kolmogorov-Smirnov tests were used to examine normal distribution of continuous variables. If normally distributed, data is presented as means  $\pm$  standard deviation (SD), otherwise as medians. We compared continuous normally-distributed data by means of paired Student's *t*-tests, while Wilcoxon signed rank and Friedman tests were performed to compare paired nonparametric variables. *P* values  $\leq 0.05$  were considered to indicate statistical significance.

## 3. Results

### 3.1. Image quality

Observers deemed all 48 ankle examinations (16 LD, 16 FD, 16 MSCT scans) suitable for diagnostic purposes. The evaluation of overall image quality was very good or excellent in 62.5/87.5/56.3% (reader 1/reader 2/reader 3; R1/R2/R3) of LD, 87.5/87.5/81.3% of FD and 100/87.5/87.5% of MSCT studies. All three observers stated that MSCT provided better overall image quality than LD scans (R1/R2/R3;  $p \leq 0.008$ ), while two observers also found significant advantages over FD imaging (R1/R3;  $p \leq 0.034$ ). Two readers evaluated FD being superior to LD image quality (R1/R3;  $p \leq 0.005$ ), while for ratings of R2 no significant difference could be observed. Fig. 2 illustrates image quality of coronally reconstructed MSCT and CBCT ankle scans.

Table 1 comprises observer ratings on subjective image quality for image noise and artifacts in bone and soft tissue. Image noise in soft tissue was significantly stronger in FD (all;  $p \leq 0.002$ ) and LD (all;  $p \leq 0.001$ ) than MDCT scans. Accordingly, image noise in bone was also more prominent in FD (all;  $p \leq 0.003$ ) and LD (all;  $p \leq 0.001$ ) studies. In addition, observers found significantly stronger artifacts in osseous tissue in FD (all;  $p \leq 0.002$ ) and LD (all;  $p < 0.001$ ) examinations. For depiction of soft tissue, MSCT also provided less artifacts than FD (all;  $p \leq 0.001$ ) and LD (all;  $p < 0.001$ ) scans. Comparing the depiction of bone and soft tissue, artifacts were stronger in soft tissue for FD (all;  $p \leq 0.014$ ) and LD (all;  $p \leq 0.025$ ). Likewise, image noise was unanimously lower in bone for FD studies (all;  $p \leq 0.014$ ).

Comparing both 3D CBCT protocols, image noise in bone was conceived unanimously lower in FD than LD (all;  $p \leq 0.005$ ) scans. In addition, two readers considered artifacts in bone tissue to be stronger in low-dose examinations (R1/R3;  $p \leq 0.020$ ).

### 3.2. Radiation dose

CTDI<sub>vol</sub>, DAP for CBCT and DLP for MSCT scans are depicted in Table 2. Mean CTDI<sub>vol</sub> was  $5.25 \pm 1.0$  mGy for FD,  $2.9 \pm 0.6$  mGy for LD and  $15.0 \pm 0.0$  mGy for MSCT scans (Fig. 3). Mean DAP in CBCT was  $40.4 \pm 7.8$  mGy\*cm<sup>2</sup> for FD and  $22.2 \pm 4.3$  mGy\*cm<sup>2</sup> for LD examinations. Mean DLP for MSCT was  $174.8 \pm 22.2$  mGy\*cm. CTDI<sub>vol</sub> was significantly lower for FD ( $p < 0.001$ ) and LD ( $p < 0.001$ ) imaging in comparison to MSCT studies. Comparing both CBCT protocols, LD was associated with significantly lower CTDI<sub>vol</sub> ( $p < 0.001$ ) and DAP ( $p < 0.001$ ) than FD scans.

## 4. Discussion

We provide a comparison between a novel X-ray system's 3D cone-beam CT function and a conventional multi-slice CT scanner with regards to image quality and radiation dose in ankle imaging. Therefore, we performed 48 scans of 16 cadaveric ankle regions using a dedicated low-dose CBCT, a standard-dose CBCT and a clinical MSCT protocol for each ankle.

Three radiologists observed that all 48 studies provided suitable image quality for diagnostic use in clinical routine. However, when comparing image quality of the three protocols, MSCT scans produced the best results for all relevant tested categories. Particularly for soft tissue, this is consistent with previous publications, as literature on extremity imaging describes more image noise and artifacts in CBCT scans. In contrast, CBCT is generally considered very good for the depiction of osseous tissue [13,18], which we can confirm for the majority of standard and low-dose scans in this study. Further endorsing this finding, the impact of artifacts and image noise on image quality proved to be higher in soft than bone tissue. Although soft tissue contrast is very important for a multitude of imaging tasks, we believe that, for ankle imaging in trauma, the depiction of bone is of superior importance to clinicians and radiologists.

Due to mismatches between the mathematical model and the actual physical imaging process, cone-beam imaging is associated with typical artifacts that are not found in MSCT scans. Since these artifacts can impact image interpretation during the diagnostic process, radiologists need to know about their existence [19]. However, adaptation may happen quickly, as observers in our study confirmed to have become familiar with the characteristic appearance of CBCT studies by the end of their reads, despite not having received any specific training beforehand.

It is well established in literature on maxillofacial imaging, that CBCT can deliver appealing image quality in bone at a favorable radiation dose over MSCT scans [11,20]. Publications on dedicated extremity scanners report similar findings for wrist [21,22], knee [23] and ankle imaging [2]. In the present study, we were able to show that the new system is also capable of producing suitable image quality for ankle studies while reducing radiation dose to approximately one third of MSCT. With the addition of a specific low-dose CBCT scan protocol, we achieved even more dose reduction with the new scanner, resulting in CTDI<sub>vol</sub> to be five times lower than in clinical MSCT imaging while maintaining diagnostic image quality.

As many younger patients are affected by ankle fractures, sometimes requiring CT imaging before surgical treatment for information on fragment displacement and involvement of articular surface, dose reduction possible with CBCT can be of particular interest for pediatric musculoskeletal radiology [24].

Under supine conditions, positioning for lower extremity 3D CBCT scans is equal to conventional MSCT. However, using the twin robotic

**Table 1**

Image quality. Evaluation of overall image quality, image noise and artifacts in osseous and soft tissue for conventional multi-slice CT (MSCT) and 3D cone-beam CT using a dedicated low-dose (LD) and standard-dose protocol (FD). Three readers performed their assessment on five-point Likert scales. Scale results are presented as frequencies (percentages) and median values.

	Likert	MSCT			FD			LD		
		R1	R2	R3	R1	R2	R3	R1	R2	R3
<b>Image quality overall</b>	5	15 (93.8)	7 (43.8)	9 (56.3)	4 (25.0)	2 (12.5)	4 (25.0)	–	–	–
	4	1 (6.3)	7 (43.8)	5 (31.3)	10 (62.5)	13 (81.3)	9 (56.3)	10 (62.5)	14 (87.5)	9 (56.3)
	3	–	2 (12.5)	2 (12.5)	2 (12.5)	1 (6.3)	3 (18.8)	6 (37.5)	2 (12.5)	4 (25.0)
	2	–	–	–	–	–	–	–	–	3 (18.8)
	1	–	–	–	–	–	–	–	–	–
	<b>Median</b>		5.0	4.0	5.0	4.0	4.0	4.0	4.0	4.0
<b>Artifacts in bone</b>	5	16 (100.0)	13 (81.3)	15 (93.8)	5 (31.3)	2 (12.5)	4 (25.0)	2 (12.5)	2 (12.5)	–
	4	–	3 (18.8)	1 (6.3)	9 (56.3)	12 (75.0)	9 (56.3)	11 (68.8)	11 (68.8)	10 (62.5)
	3	–	–	–	2 (12.5)	2 (12.5)	3 (18.8)	1 (6.3)	3 (18.8)	6 (37.5)
	2	–	–	–	–	–	–	2 (12.5)	–	–
	1	–	–	–	–	–	–	–	–	–
	<b>Median</b>		5.0	5.0	5.0	4.0	4.0	4.0	4.0	4.0
<b>Artifacts in soft tissue</b>	5	15 (93.8)	13 (81.3)	14 (87.5)	–	–	1 (6.3)	–	–	–
	4	1 (6.3)	3 (18.8)	2 (12.5)	1 (6.3)	4 (25.0)	7 (43.8)	1 (6.3)	6 (37.5)	6 (37.5)
	3	–	–	–	12 (75.0)	12 (75.0)	8 (50.0)	9 (56.3)	10 (62.5)	9 (56.3)
	2	–	–	–	3 (18.8)	–	–	6 (37.5)	–	1 (6.3)
	1	–	–	–	–	–	–	–	–	–
	<b>Median</b>		5.0	5.0	5.0	3.0	3.0	4.0	3.0	3.0
<b>Image noise in bone</b>	5	15 (93.8)	12 (75.0)	14 (87.5)	6 (37.5)	1 (6.3)	2 (12.5)	2 (12.5)	–	–
	4	1 (6.3)	4 (25.0)	2 (12.5)	7 (43.8)	15 (93.8)	12 (75.0)	8 (50.0)	9 (56.3)	2 (12.5)
	3	–	–	–	3 (18.8)	–	2 (12.5)	4 (25.0)	7 (43.8)	13 (81.3)
	2	–	–	–	–	–	–	2 (12.5)	–	1 (6.3)
	1	–	–	–	–	–	–	–	–	–
	<b>Median</b>		5.0	5.0	5.0	4.0	4.0	4.0	4.0	4.0
<b>Image noise in soft tissue</b>	5	2 (12.5)	10 (62.5)	12 (75.0)	–	1 (6.3)	–	–	–	–
	4	14 (87.5)	6 (37.5)	4 (25.0)	1 (6.3)	9 (56.3)	5 (31.3)	–	4 (25.0)	–
	3	–	–	–	11 (68.8)	6 (37.5)	11 (68.8)	8 (50.0)	10 (62.5)	14 (87.5)
	2	–	–	–	4 (25.0)	–	–	8 (50.0)	2 (12.5)	2 (12.5)
	1	–	–	–	–	–	–	–	–	–
	<b>Median</b>		4.0	5.0	5.0	3.0	4.0	3.0	2.5	3.0

**Table 2**

Radiation dose. Dose estimation for conventional multi-slice CT using a clinical scan protocol (MSCT) and 3D cone-beam CT (CBCT) using a dedicated low-dose (LD) and standard-dose (FD) protocol. Mean values and standard deviations of volume computed tomography indices (CTDI<sub>vol</sub>) are presented for both CBCT protocols and the conventional MSCT protocol.

Parameters	MSCT	FD	LD	p value
CTDI <sub>vol</sub> (mGy)	15.0 ± 0.0	5.3 ± 1.0	2.9 ± 0.6	≤ 0.001
DAP (mGy x cm <sup>2</sup> )	–	40.4 ± 7.8	22.2 ± 4.3	≤ 0.001
DLP (mGy x cm)	367.1 ± 46.7	–	–	–

X-ray system, additional weight-bearing imaging may also be feasible. This option may be particularly appealing for ankle studies, as depiction of syndesmosis varies considerably depending on the axial load [16]. Additional imaging tasks that profit from weight-bearing positioning may include scans of the knee joint [17] and lumbar spine [14]. Another promising application could be the option to perform direct CT arthrography of the lower tibiofibular joint. Using the systems' fluoroscopy mode to control the articular injection of contrast agent, the patient could remain in position for the acquisition of CT images. With conventional MSCT or MRI arthrography, the latter being the preferred method today, the fluoroscopy-controlled injection has to be performed in a different room, resulting in repeated positioning of the patient and presumably increased scheduling effort. CBCT arthrography of the wrist has been shown to deliver excellent spatial resolution and more accurate depiction of articular cartilage lesions than MRI arthrography [25,26]. However, to the authors' best knowledge, no literature on CBCT arthrography of the ankle has been published to date.

4.1. Limitations

We evaluated 16 formalin-fixated cadaveric ankle regions from eight body donors. Formalin fixation is known to accelerate the demineralization of osseous tissue over time [27,28] which might have caused a subjective decrease in image quality in some ankles. As only human cadaveric specimens were examined in this study, the possibility of motion artifacts has to be considered for patient scans given the acquisition time of 20 s with the new scanner. Due to comfortable positioning, patients may tolerate the longer scan time without considerable increase of motion artifacts, when properly fixated. However, extrapolation for suitability in clinical ankle imaging cannot be made and the actual advantage of the new system might be less pronounced in a clinical setting with lower soft tissue resolution and higher image noise in CBCT scans.

Observers did not receive any particular training on CBCT imaging before this study and were blinded to the type of image they rated. Nonetheless, the typical image appearance of CBCT images may have imposed a certain level of bias.

Finally, we compared results of the twin robotic X-ray system to a MSCT scanner using a clinical protocol. Therefore, automatic tube current modulation was inactive in conventional MSCT scans. As the current software version for the multi-use X-ray system does not support the manual deactivation of automatic dose modulation, future work should include similar modulation setups for scanners to achieve optimal comparability. Furthermore, MSCT studies should also be conducted using a dedicated low-dose scan protocol to evaluate image quality and radiation dose.

5. Conclusion

Despite MSCT scans providing better overall image quality in this

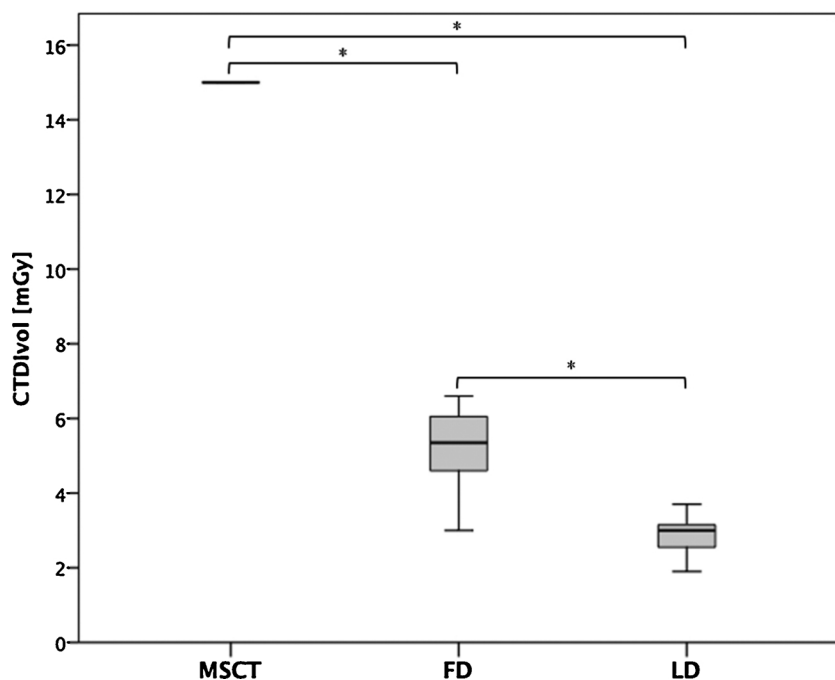


**Fig. 3.** Radiation dose comparison. Volume computed tomography dose indices (CTDIvol) for conventional multi-slice (MSCT) and 3D cone-beam CT imaging (FD = standard-dose protocol; LD = low-dose protocol). Boxplots (median and inter-quartile-range) illustrate CTDIvol differences [mGy] between scan protocols. Asterisks (\*) indicate statistical significance ( $p < 0.001$ ).

study, the twin robotic X-ray system’s 3D CBCT mode delivers acceptable image quality in the majority of examinations. While image noise and typical artifacts are primarily present in soft tissue, overall image quality of 3D CBCT scans in this study is consistently suitable for clinical ankle imaging, irrespective of the selected dose level. Furthermore, both CBCT scan protocols may enable substantial dose reduction, as standard-dose and low-dose CBCT studies were associated with approximately three respectively five times less radiation than the clinical scan protocol of a conventional MSCT scanner. With additional radiography and fluoroscopy options, the tested system may potentially serve as a one-stop-shop device for trauma-associated ankle imaging.

**Disclaimer**

Siemens Healthineers Multitom Rax is not commercially available in all countries. Its future availability cannot be guaranteed.

**Funding**

The Department of Diagnostic and Interventional Radiology of the University Hospital Würzburg received a financial research grant by Siemens Healthineers.

Jan-Peter Grunz was financially supported by the Interdisciplinary Center of Clinical Research Würzburg [grant number Z-2/CSP-06].

**References**

[1] S.E. Lamb, J.L. Marsh, J.L. Hutton, R. Nakash, M.W. Cooke, Mechanical supports for acute, severe ankle sprain: a pragmatic, multicentre, randomised controlled trial, *Lancet* (2009), [https://doi.org/10.1016/S0140-6736\(09\)60206-3](https://doi.org/10.1016/S0140-6736(09)60206-3).  
 [2] J. Koivisto, T. Kiljunen, N. Kadesjö, X.Q. Shi, J. Wolff, Effective radiation dose of a MSCT, two CBCT and one conventional radiography device in the ankle region, *J. Foot Ankle Res.* 8 (2015), <https://doi.org/10.1186/s13047-015-0067-8>.  
 [3] C.M. Court-Brown, B. Caesar, Epidemiology of adult fractures: a review, *Injury* 37 (2006) 691–697, <https://doi.org/10.1016/j.injury.2006.04.130>.  
 [4] V. Roberts, L.W. Mason, E. Harrison, A.P. Molloy, J. Mangwani, Does functional outcome depend on the quality of the fracture fixation? Mid to long term outcomes of ankle fractures at two university teaching hospitals, *Foot Ankle Surg.* (2018) doi:10.1016/j.fas.2018.04.008 [Epub ahead of print].  
 [5] T.J. Mosher, B.N. Weissman, M.A. Bruno, R. Adler, M.E. Dempsey, S.A. Bernard, B. Khurana, F.D. Beaman, R.J. Ward, M. Appel, I.B. Fries, V. Khoury, C.C. Roberts, M.J. Tuite, M.J. Kransdorf, A.C. Zoga, ACR appropriateness criteria acute trauma to the ankle, *J. Am. Coll. Radiol.* (2015), <https://doi.org/10.1016/j.jacr.2014.11.015>.  
 [6] M. Carrozzo, G. Vicenti, V. Pesce, G. Solarino, F. Rifino, A. Spinarelli, C. Campagna,

D. Bizzoca, B. Moretti, Beyond the pillars of the ankle: a prospective randomized CT analysis of syndesmosis’ injuries in Weber B and C type fractures, *Injury* (2018), <https://doi.org/10.1016/j.injury.2018.10.005>.  
 [7] D.J. Brenner, E.J. Hall, Computed tomography — an increasing source of radiation exposure, *N. Engl. J. Med.* 357 (2007) 2277–2284, <https://doi.org/10.1056/NEJMr072149>.  
 [8] H. Matikka, T. Virén, Radiation dose reduction in cone-beam computed tomography of extremities: evaluation of a novel radiation shield, *J. Radiol. Prot.* (2014), <https://doi.org/10.1088/0952-4746/34/2/N57>.  
 [9] B. Koong, Cone beam imaging: is this the ultimate imaging modality? *Clin. Oral Implants Res.* 21 (2010) 1201–1208, <https://doi.org/10.1111/j.1600-0501.2010.01996.x>.  
 [10] K. Tsiklakis, C. Donta, S. Gavala, K. Karayianni, V. Kamenopoulou, C.J. Hourdakis, Dose reduction in maxillofacial imaging using low dose Cone Beam CT, *Eur. J. Radiol.* 56 (2005) 413–417, <https://doi.org/10.1016/j.ejrad.2005.05.011>.  
 [11] J.A. Roberts, N.A. Drage, J. Davies, D.W. Thomas, Effective dose from cone beam CT examinations in dentistry, *Br. J. Radiol.* (2009), <https://doi.org/10.1259/bjr/31419627>.  
 [12] F. Lintz, C. de Cesar Netto, A. Barg, A. Burssens, M. Richter, Weight Bearing CT International Study Group, weight-bearing cone beam CT scans in the foot and ankle, *EFORT Open Rev.* (2018), <https://doi.org/10.1302/2058-5241.3.170066>.  
 [13] J.A. Carrino, A. Al Muhit, W. Zbijewski, G.K. Thawait, J.W. Stayman, N. Packard, R. Senn, D. Yang, D.H. Fooks, J. Yorkston, J.H. Siewerdsen, Dedicated cone-beam CT system for extremity imaging, *Radiology* 270 (2014) 816–824, <https://doi.org/10.1148/radiol.13130225>.  
 [14] R.M. Benz, D. Harder, F. Amsler, J. Voigt, A. Fieselmann, A.L. Falkowski, B. Stieltjes, A. Hirschmann, Initial assessment of a prototype 3D cone-beam computed tomography system for imaging of the lumbar spine, evaluating human cadaveric specimens in the upright position, *Invest. Radiol.* 53 (2018) 714–719, <https://doi.org/10.1097/RLL.0000000000000495>.  
 [15] A. Hirschmann, C.W.A. Pfirrmann, G. Klammer, N. Espinosa, F.M. Buck, Upright Cone CT of the hindfoot: comparison of the non-weight-bearing with the upright weight-bearing position, *Eur. Radiol.* 24 (2014) 553–558, <https://doi.org/10.1007/s00330-013-3028-2>.  
 [16] K. Malhotra, M. Welck, N. Cullen, D. Singh, A.J. Goldberg, The effects of weight bearing on the distal tibiofibular syndesmosis: a study comparing weight bearing-CT with conventional CT, *Foot Ankle Surg.* (2018), <https://doi.org/10.1016/j.fas.2018.03.006>.  
 [17] E.K.J. Tuominen, J. Kankare, S.K. Koskinen, K.T. Mattila, Weight-bearing CT imaging of the lower extremity, *Am. J. Roentgenol.* (2013), <https://doi.org/10.2214/AJR.12.8481>.  
 [18] S. Demehri, A. Muhit, W. Zbijewski, J.W. Stayman, J. Yorkston, N. Packard, R. Senn, D. Yang, D. Fooks, G.K. Thawait, L.M. Fayad, A. Chhabra, J.A. Carrino, J.H. Siewerdsen, Assessment of image quality in soft tissue and bone visualization tasks for a dedicated extremity cone-beam CT system, *Eur. Radiol.* 25 (2015) 1742–1751, <https://doi.org/10.1007/s00330-014-3546-6>.  
 [19] R. Schulze, U. Heil, D. Groß, D.D. Bruellmann, E. Dranschnikow, U. Schwanecke, E. Schoemer, Artefacts in CBCT: a review, *Dentomaxillofacial Radiol.* (2011), <https://doi.org/10.1259/dmfr/30642039>.  
 [20] S. Veldhoen, M. Schöllchen, H. Hanken, C. Precht, F.O. Henes, G. Schön, H.D. Nagel, U. Schumacher, M. Heiland, G. Adam, M. Regier, Performance of cone-beam computed tomography and multidetector computed tomography in diagnostic

- imaging of the midface: a comparative study on Phantom and cadaver head scans, *Eur. Radiol.* 27 (2017) 790–800, <https://doi.org/10.1007/s00330-016-4387-2>.
- [21] J. Koivisto, M. van Eijnatten, T. Kiljunen, X.Q. Shi, J. Wolff, Effective radiation dose in the wrist resulting from a radiographic device, two CBCT devices and one MSCT device: a comparative study, *Radiat. Prot. Dosimetry* 179 (2018) 58–68, <https://doi.org/10.1093/rpd/ncx210>.
- [22] N. Faccioli, G. Foti, M. Barillari, A. Atzei, R.P. Mucelli, Finger fractures imaging: accuracy of cone-beam computed tomography and multislice computed tomography, *Skeletal Radiol.* 39 (2010) 1087–1095, <https://doi.org/10.1007/s00256-010-0911-7>.
- [23] J. Koivisto, T. Kiljunen, J. Wolff, M. Korteniemi, Assessment of effective radiation dose of an extremity CBCT, MSCT and conventional X-ray for knee area using MOSFET dosimeters, *Radiat. Prot. Dosimetry* 157 (2013) 515–524, <https://doi.org/10.1093/rpd/nct162>.
- [24] S. Tschauener, R. Marterer, E. Nagy, G. Apfaltrer, M. Riccabona, G. Singer, G. Stucklschweiger, H. Guss, E. Sorantin, Surface radiation dose comparison of a dedicated extremity cone beam computed tomography (CBCT) device and a multidetector computed tomography (MDCT) machine in pediatric ankle and wrist phantoms, *PLoS One* (2017), <https://doi.org/10.1371/journal.pone.0178747>.
- [25] N. Suojärvi, V. Haapamäki, N. Lindfors, S.K. Koskinen, Radiocarpal injuries: cone beam computed tomography arthrography, magnetic resonance arthrography, and arthroscopic correlation among 21 patients, *Scand. J. Surg.* 106 (2017) 173–179, <https://doi.org/10.1177/1457496916659226>.
- [26] S.K. Koskinen, V.V. Haapamäki, J. Salo, N.C. Lindfors, M. Korteniemi, L. Seppälä, K.T. Mattila, CT arthrography of the wrist using a novel, mobile, dedicated extremity cone-beam CT (CBCT), *Skeletal Radiol.* 42 (2013) 649–657, <https://doi.org/10.1007/s00256-012-1516-0>.
- [27] A.A. Fonseca, K. Cherubini, E.B. Veeck, R.S. Ladeira, L.P. Carapeto, Effect of 10% formalin on radiographic optical density of bone specimens, *Dentomaxillofacial Radiol.* (2008), <https://doi.org/10.1259/dmfr/18109064>.
- [28] K.J. Burkhart, T.E. Nowak, J. Blum, S. Kuhn, M. Welker, W. Sternstein, L.P. Mueller, P.M. Rommens, Influence of formalin fixation on the biomechanical properties of human diaphyseal bone, *Biomed. Tech.* (2010), <https://doi.org/10.1515/BMT.2010.043>.